Research of effective thermal conductivity and its parts in porous metallic materials with different parameters of porosity

Pavlenko A.M.

Doctor of Technical Sciences, Professor Department of Building Physics and Renewable Energy
Kielce University of Technology, Poland,
E-mail: am.pavlenko@i.ua

Koshlak H.V.

PhD, Associate Professor Department of heat and gas supply, ventilation and heat power engineering Poltava national technical Yuri Kondratyuk university

Cheilytko A.O.

PhD, Associate Professor Department of heat and power engineering
Zaporizhzhya state engineering academy

Nosov M.A.

Department of heat and power engineering
Zaporizhzhya state engineering academy

Syzonenko A.V.

Department of oil and gas fields equipment
Poltava national technical Yuri Kondratyuk university

Abstract
In this article, an analysis of impact of the form, size and location of pores on the effective thermal conductivity coefficient of porous metallic materials is presented. It is shown the influence of porosity parameters separately on the electronic and phonon; convective and radiation component of effective thermal conductivity. The distribution of the heat flow and temperature in the experimental samples were analyzed. Form and location of pores, which give opportunity to reached minimum electronic and phonon thermal conductivity, and also the most significant factor (porosity parameter), which influence on the electronic and phonon thermal conductivity are found. The previously expressed hypothesis about the impact on the convective motions by not only pores size, but also temperature is confirmed. Dependence of convective and radiation heat conductivity from the pores size in the porous metal material was obtained.
Key words: EFFECTIVE THERMAL CONDUCTIVITY, PHONON THERMAL CONDUCTIVITY, RADIATION THERMAL CONDUCTIVITY, CONVECTION THERMAL CONDUCTIVITY, POROUS PARAMETERS, ALLOCATION OF HEAT FLOW

Introduction

The metals porosity, which reduces the mechanical properties and tightness of the material, has been perceived only as a negative factor for a long time. For preventing and blocking the negative effects of porosity in metals, a lot of scientific works were dedicated; some of them are used in present time [1-3].

Despite the negative impact of porosity, porous metal materials found use in various fields: in the aerospace industry as titanium and aluminum sandwich panels; in medicine as implants in humans [4]; in shipbuilding as a body for passenger vessels; in the automotive industry as structural elements [5-7]. Prevalence of porous metallic materials is caused by their unique physical and mechanical characteristics such as high stiffness in combination with a very low density (low specific gravity) and / or high gas permeability combined with a high / low thermal conductivity [8]. Such materials can be globally divided into three types: porous metals [9]; metallic foams [10, 11] and cellular metals [12-13]. Each category has its unique porosity parameters and methods of production.

In spite of the unique characteristics and prevalence of porous metal materials, the unified theory of dependence of the effective thermal conductivity from the parameters of porosity (pores location, pores form, their size, etc.) is still lacking without mentioning the influence of these parameters on the electronic and phonon, convective and radiation parts of effective thermal conductivity [13].

The main part of research

Electronic thermal conductivity in physical metallic samples

For research of electronic thermal conductivity, Wiedemann-Franz law was chosen. This law is based on the thermo-electrical analogy and can be used only for metallic materials. After numerous changes finite equation, which characterizes the Wiedemann-Franz law, is

$$\frac{\lambda}{\sigma} = \frac{\pi^2}{3} \cdot \left(\frac{k_B}{e}\right)^2 \cdot T,$$

where $\frac{\pi^2}{3} \cdot \left(\frac{k_B}{e}\right)^2$ = L - Lorenz number, $W \cdot \Omega \cdot K^{-2}$.

Theoretically Lorenz number for all metals is equal to $2.44 \cdot 10^{-8}$ $W \cdot \Omega \cdot K^{-2}$. But on practice it is not true. Because in real metallic materials, there are a lot of impurities, which provoke the additional scattering of electrons on impurity atoms.

That is why, it was decided to use the following formula to calculate Lorenz number

$$L = \frac{\lambda}{T \cdot \sigma},$$

where λ - coefficient of thermal conductivity, W / (m·K);

T - temperature, at which coefficient of thermal conductivity was taken, K;

σ - coefficient of specific electrical conductivity, S/m.

Since we know the material from which sample is made, there is only one unknown variable - coefficient of specific electrical conductivity, which can be found by the following formula

$$\sigma = \frac{1}{\rho_v} = \frac{l}{R \cdot S} = \frac{I \cdot l}{U \cdot S},$$

where I - current intensity, A;

U - electric potential difference, V;

l - sample length, m;

S - cross sectional area of sample, m^2.

For finding current intensity and electric potential difference, experimental installation was made, circuitry of which can be seen in Figure 1.

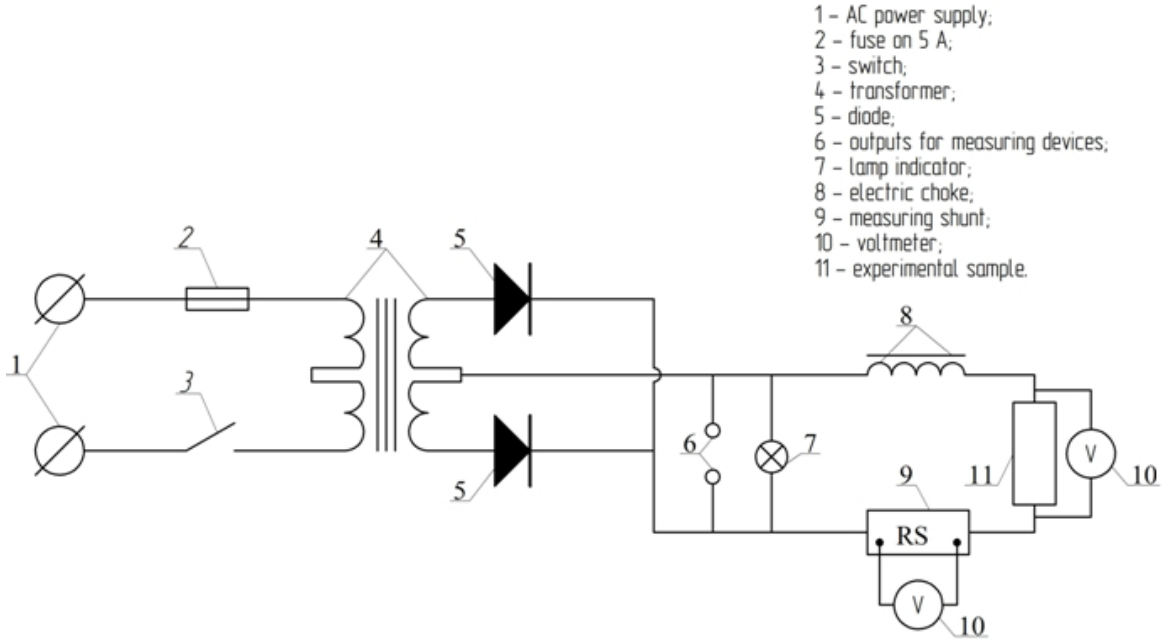

Figure 1. Circuitry of experimental installation

As experimental samples, stainless steel plates and copper plates were chosen. In the plates, perforation was carried out with different diameters: for stainless steel plates 3.2-15 mm; for copper plates 4-20 mm. To explore the influence of pores location on the electronic thermal conductivity, in-line and staggered location of holes was used. Stainless steel plates with in-line and staggered location of holes can be seen in Figure 2.

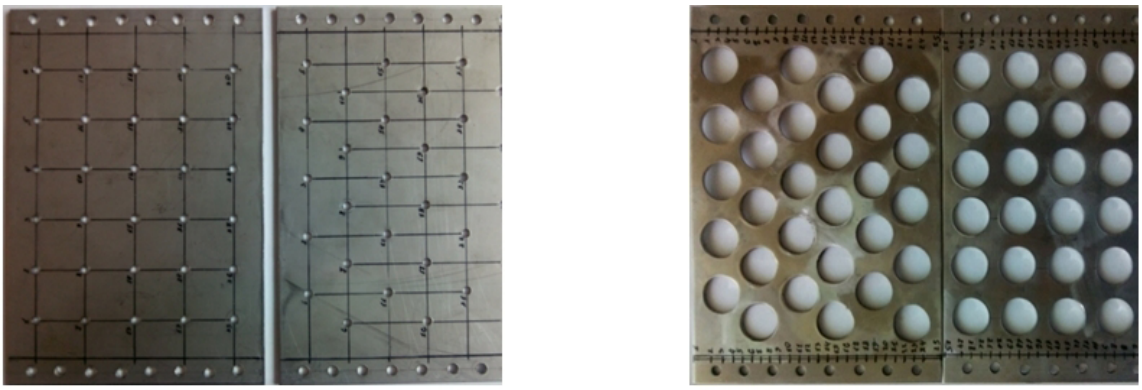

Figure 2. Stainless steel plates with in-line and staggered location of holes, with diameters 3.2 and 15 mm

Data obtained during the experiments on stainless steel and copper samples were presented in Table 1, where λ_l – coefficient of thermal conductivity for samples with in-line location holes, λ_s – for samples with staggered location holes.

Electronic and phonon thermal conductivity in three-dimensional samples

All subsequent experiments are based on the computer modeling method. Such choice is substantiated by the fact that the manufacturing of metal samples with different precise forms is extremely difficult and can lead to some errors of results; computer method give chance to research effective thermal conductivity as well as only electron and photon thermal conductivity.

For computer modeling, special software was used. Parameters of three-dimension models are fully comply with the parameters of their physical analogs (Fig. 3).

For modeling thermal processes, the following values were used:

– heat flow, 0.1 W;

– ambient temperature and samples temperature, 20 ° C;

– heat transfer coefficient, 23 W/m^2·K;

– heating time, 1 second;

– convective surface located opposite the heating surface, other surfaces adiabatic.

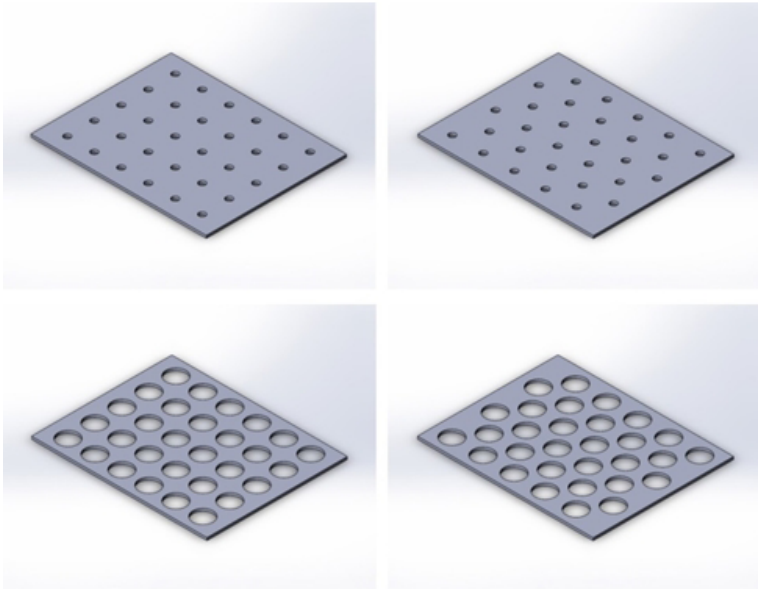

Figure 3. Three-dimensional models of stainless steel samples with diameters of holes 5 and 15 mm

Before modeling of thermal process, every prototype had been divided by ~ 250 000 elements with a cubic grid, size of one such element was 0.0004 m. After finishing process, we have had temperatures of heating and opposite surfaces in the last moment of time. Thermal conductivity coefficient can be calculated by next formula

$$\lambda = \frac{Q \cdot l}{(T_2 - T_1) \cdot S},$$

where I - sample length, m;

Q - heat flow, W;

T_1, T_2 – temperatures of heating and opposite surfaces, K;

S – cross sectional area of sample, m^2.

Data obtained during the experiments on stainless steel and copper three-dimension models were presented in Table 2. By results from Tables 1 and 2, dependences of the thermal conductivity coefficient of the holes diameter were built (Fig. 4, 5).

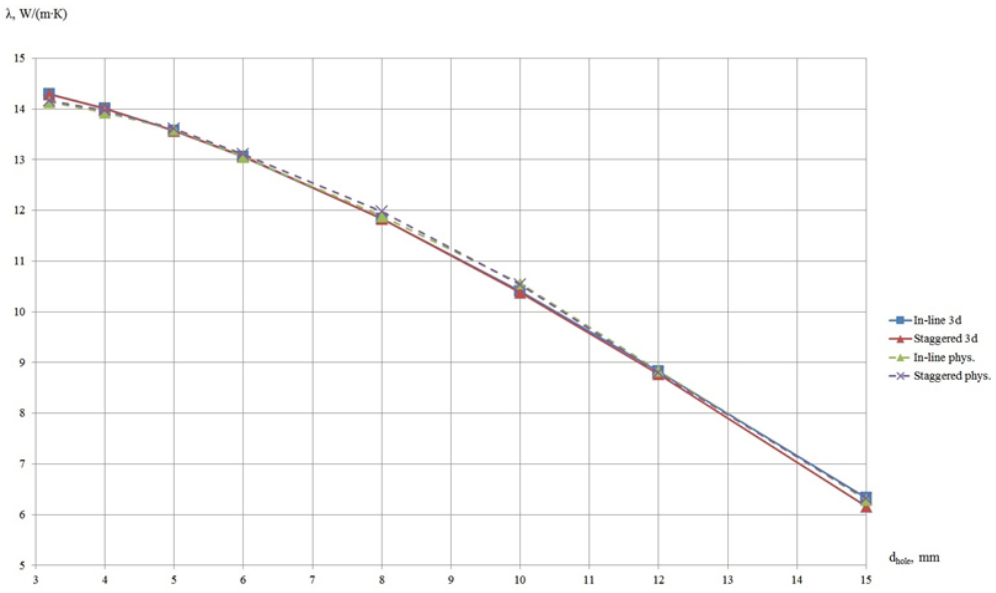

Figure 4. Dependence of the thermal conductivity coefficient of the holes diameter for stainless steel samples

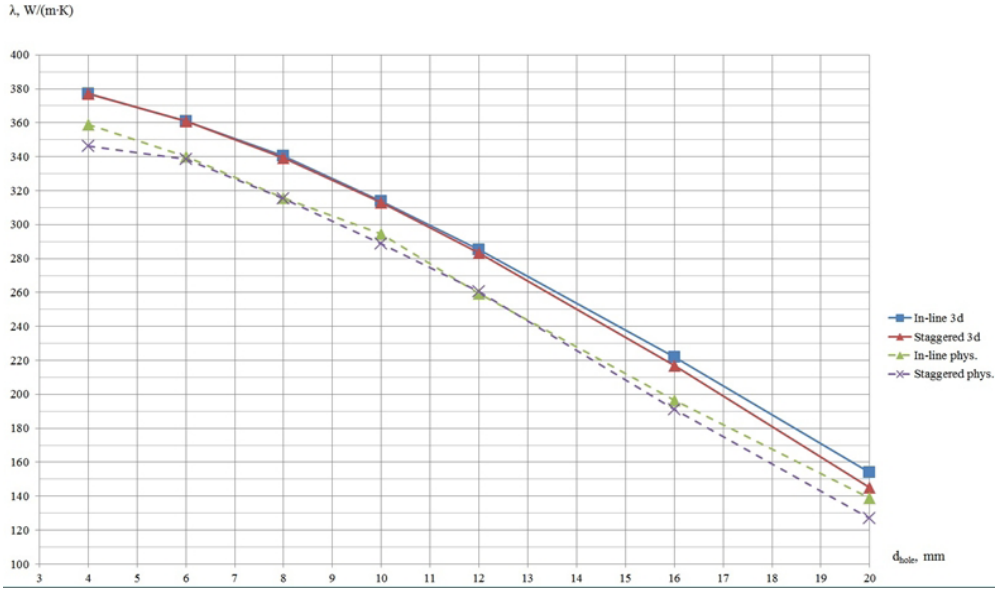

Figure 5. Dependence of the thermal conductivity coefficient of the holes diameter for copper samples

In Figures 4 and 5, we can see that general character of dependence is equal for computer and physical method. Difference of results in copper samples is caused by the fact that the thermal conductivity of copper is higher and phonon thermal conductivity begins to increase with lower temperatures than in steel. Also this results show us that computer method give truly information and can be used in the further researches.

For researching the influence of the pores form on the thermal conductivity, three-dimensional models were made with the following perforation forms: hexagon, equilateral triangle, square, ellipse and circle. Cross-sectional area for each hole was the same and equaled $1.13094 \cdot 10^{-4}$ m^2, this step gave us identical porosity in all samples. Like in previous experiment, holes location was in-line and staggered, parameters for thermal modeling were the same. Stainless steel was chosen as material for samples. Allocation of temperature is shown in Fig. 6, 7.

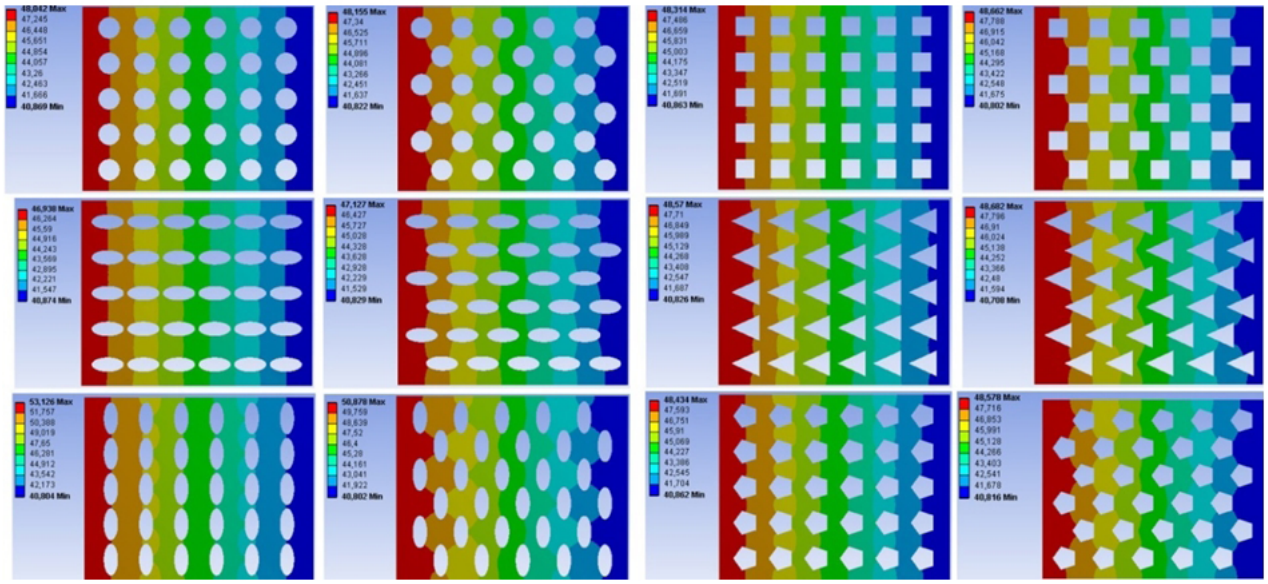

Figure 6. Temperature allocation in the three-dimensional models

Obtained results were presented in Table 3. In Figure 6, we can see diagram which was built by this results. For ellipse 1, the case when a large diagonal of the ellipse is parallel to the heat flow was accepted, and for ellipse 2 - when perpendicular to the heat flow. Diagram shows us main laws of influence of pores form on electronic and phonon thermal conductivity. After analyzing data, we can confidently assert that pores form make greater impact on the electronic and phonon thermal conductivity than their location (at the

same porosity). The lowest thermal conductivity was achieved by using the elliptic form pores with in-line location. The reason of this result is the shortest distance between the pores, which causes maximum heat dissipation (among all other samples), which is transferred by the conduction electrons. All previous results show us that pores form is the most important for developing porous metallic materials.

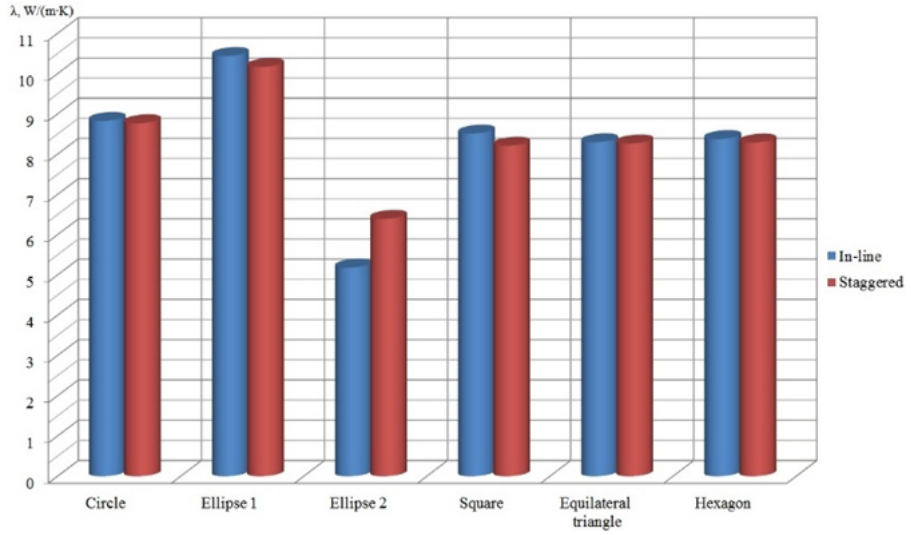

Figure 7. Thermal conductivity coefficients for three-dimensional models with different perforation forms

Effective thermal conductivity in three-dimensional samples

To investigate the changes of effective thermal conductivity coefficient three-dimensional models were created as before, but this time with the presence of air in the holes, that will allow us to take into account the radiation and convective components of thermal conductivity. In Figure 8, we can see sample grid with air in the holes. The number of elements was about 550 000. The number of units was more than two million. Cubic mesh was taken with automatic choice of proximity and curvature elements. The value of smooth and relevance of centers elements is average. The method of construction is automatic mechanical with complicated parallel construction. Thermal properties correspond to stainless steel, the material in the holes is air.

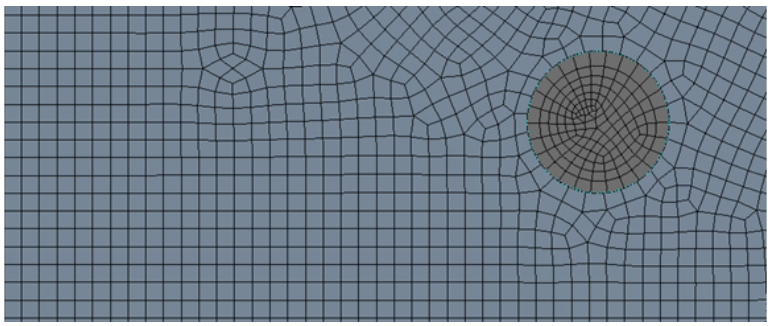

Figure 8. Part of mesh of three-dimensional models with air in the holes

Obtained data are presented in Table 4. It should be noted, that the air in holes create extra outlets of heat, since heat capacity of air is twice higher than heat capacity of the metal. Therefore, the temperatures at the ends of samples with considering convection and radiation are lower than temperatures of samples with adiabatic surfaces in the holes.

Convective and radiation thermal conductivity in three-dimension samples

Based on obtained data (Table 3, 4), dependency of convective and radiation thermal conductivity from the effective thermal conductivity was built (Fig. 9). Convective and radiation thermal conductivity was found by deducting the electron and phonon component from the effective heat conduction.

In Figure 8, we can clearly see the difference between radiation and convective thermal conductivity for pores with in-line and staggered location. This is due to various changes of temperature on the holes boundaries.

Allocation of the heat flow in three-dimensional samples with air in the pores (diameter of holes is 8 mm) is shown in Figure 9.

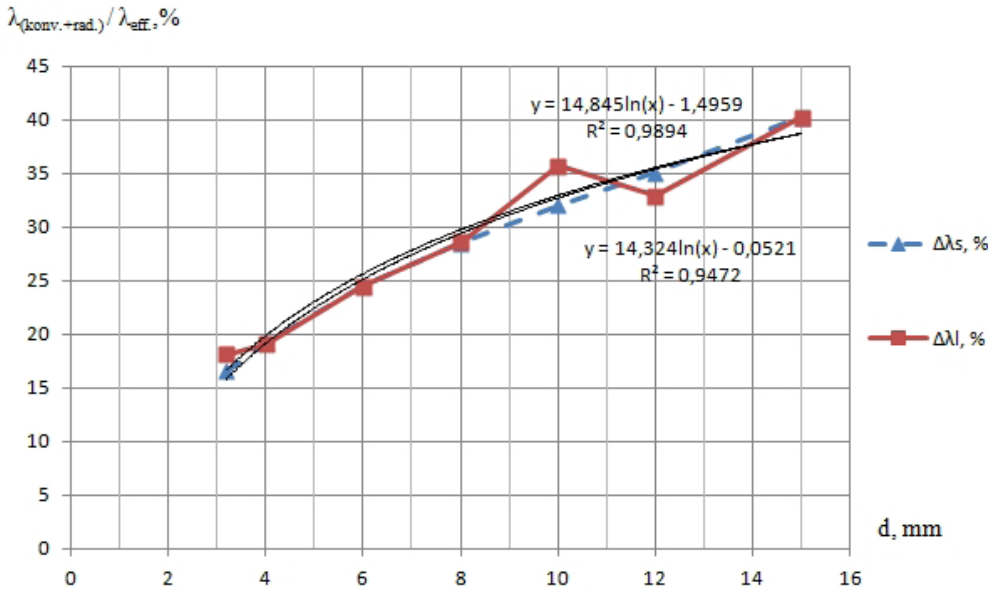

Figure 9. Dependency of convective and radiation thermal conductivity from the effective thermal conductivity for three-dimensional models

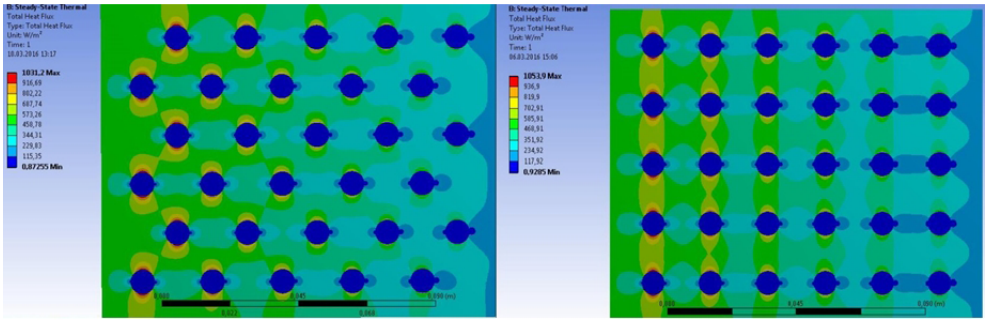

Figure 10. Allocation of the heat flow in three-dimensional samples with air in the pores, diameter of holes is 8 mm

As we can see in Figure 10, the lowest heat flow is observed in the holes with air. When thermal resistance is growing, the heat flow decreases. The maximum temperature gradient is directed to the shortest distance between the pores, this will be increasing the convection in this direction. Thus, in the samples with staggered location holes, convection in the holes will be maximum at 45° to the direction of heat flow (Fig. 11a).

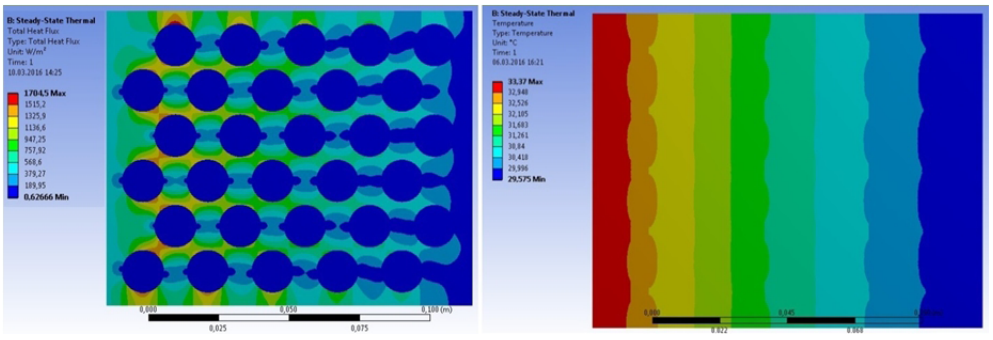

a) b)

Figure 11. Allocation of the: a) heat flow in sample with staggered located holes (diameter is 15 mm); b) temperature in sample with in-line located holes (diameter is 8 mm)

Figure 11b shows us that temperature of air in the holes is allocated evenly; at temperatures over 31 ^{0}C in the holes 8 mm, air facilitates transferring the heat (by convection) and at lower temperatures, it increases the thermal resistance (convection is very low or absent). This confirms the previously expressed hypothesis about the impact of not only pores size, but also temperature on the convective motions. Analogical computer modeling was made with copper and aluminum samples. General dependences of convective and radiation thermal conductivity on effective thermal conductivity remained the same. In percentage, convective and radiation part of the thermal conductivity is lowest in copper 14% (with holes 15 mm) due to the high thermal conductivity of copper.

Results of research

Table 1. Electron thermal conductivity coefficients for the stainless steel and copper samples

d, mm	λ_l, W/(m·K)	λ_s, W/(m·K)
Stainless steel		
3,2	14.137	14.158
4	13.926	13.969
5	13.592	13.607
6	13.055	13.107
8	11.891	11.971
10	10.560	10.532
12	8.842	8.803
15	6.294	6.314
Copper		
4	358.8480	346.0934
6	340.0536	338.5800
8	315.8059	315.4422
10	294.6443	288.6011
12	259.4194	260.4277
16	196.4911	190.8948
20	139.0258	127.1524

Table 2. Electron and phonon thermal conductivity coefficients for the stainless steel and copper three-dimensional models

d, mm	T_1, °C	T_2, °C	λ_l, W/(m·K)	T_1, °C	T_2, °C	λ_s, W/(m·K)
Stainless steel						
3.2	40.906	45.281	14.2857	40.91	45.284	14.2889
4	40.907	45.371	14.0009	40.914	45.375	14.0103
5	40.91	45.515	13.5722	40.92	45.524	13.5751
6	40.913	45.699	13.0589	40.928	45.711	13.0671
8	40.922	46.204	11.8326	40.949	46.232	11.8304
10	40.938	46.947	10.4010	40.982	47.002	10.3820
12	40.962	48.042	8.8276	41.028	48.155	8.7694
15	41.04	50.924	6.3233	41.146	51.28	6.1673
Copper						
4	55.135	55.467	377.2666	55.135	55.467	377.2666

6	55.135	55.482	360.9583	55.136	55.483	360.9583
8	55.137	55.505	340.3601	55.137	55.506	339.4377
10	55.138	55.537	313.9161	55.139	55.539	313.1313
12	55.141	55.58	285.3133	55.142	55.584	283.3768
16	55.151	55.715	222.0789	55.151	55.728	217.0754
20	55.176	55.99	153.8729	55.171	56.035	144.9682

Table 3. Thermal conductivity coefficients for three-dimensional models with different perforation forms

Perforation form	λ_l, W/(m·K)	λ_s, W/(m·K)
Circle	8.8277	8.7695
Ellipse 1	10.4393	10.1692
Ellipse 2	5.1833	6.3952
Square	8.5127	8.2118
Equilateral triangle	8.2968	8.2683
Hexagon	8.3769	8.2902

Table 4. Effective thermal conductivity coefficients for three-dimensional models with the air in the holes

In-line location				Staggered location		
d, mm	T_1, °C	T_2, °C	λ_l, W/(m·K)	T_1, °C	T_2, °C	λ_s, W/(m·K)
3,2	34.334	37.918	17.4386	34.295	37.944	17.128
4	33.241	36.853	17.3034	33.183	36.786	17.3467
6	31.166	34.784	17.2747	31.185	34.796	17.3082
8	29.596	33.37	16.5606	29.626	33.403	16.5475
10	26.865	30.73	16.1707	28.366	32.459	15.27
12	28.314	33.064	13.1578	27.303	31.93	13.5077
15	25.835	31.74	10.5842	25.844	31.903	10.3152

Conclusions

Based on obtained results the following conclusions were made:

1. Pores form has greater effect on electronic and phonon thermal conductivity than their location.

2. In samples with elliptic pores and their staggered location, differences between parallel and perpendicular location to heat flow was 59 %.

3. If we change circular holes into elliptic holes, which are located perpendicular to the heat flow, thermal conductivity coefficient will decrease by 27 %.

4. Thermal conductivity of the samples with holes forms of a hexagon, equilateral triangle and square is almost equal and lower than at circular form by 3.56-6%.

5. According to the results of computer simulation, the maximum convection and radiation part of effective thermal conductivity was 40.25% (with a holes diameter is 15 mm).

6. In samples with different diameters of holes, average convective and radiation effect was 24.69% from effective thermal conductivity.

7. In sample with holes diameter 15 mm and in-line location, convective and radiation part of the effective thermal conductivity increases the effective thermal conductivity by 4.26 W/(m · K), and staggered location – by 4.15 W / (m · K).

8. Maximum temperature gradient is directed along the shortest distance between the pores and it increases the convection in this direction.

References

1. Gunasegaram D. R., Farnsworth D. J., Nguyen T. T. (2009) Identification of critical factors affecting shrinkage porosity in permanent mold casting

using numerical simulations based on design of experiments. *Materials Processing Technology*. Vol. 209, p.p. 1209-1219.
2. Spasskij A. G. (1950) *Osnovy litejnogo proizvodstva* [Fundamentals of foundry]. Moscow: Metallurgizdat. 318 p.
3. Impregnation improves casting quality. *Vacuum*. 1953. Vol. 3, No 1, p.p. 94.
4. William van Grunsven (2014) Porous metal implants for enhanced bone ingrowth and stability. *Thesis submitted to the University of Sheffield for the degree of Doctor of Philosophy*. Department of Materials Science and Engineering. September 2014.
5. Reglero J. A., Rodriguez-Perez M. A., Solorzano E., J. A. de Saia (2011) Aluminium foams as a filler for leading edges: Improvements in the mechanical behavior under bird strike impact tests. *Materials and design*. Vol. 32, No 2, p.p. 907-910.
6. Lepeshkin I. A., Ershov M. Ju. (2010) Vspenennyj aljuminij v avtomobilestroenii [Foamed aluminum in automobile industry]. *Avtomobil'naja promyshlennost'* [Automobile industry]. No 10, p.p. 36-39.
7. Krupin Ju. A., Avdeenko A. M. (2008) Sil'noporistye struktury – novyj klass konstrukcionnyh materialov [Highly porous structure as a new class of structural materials]. *Tjazheloe mashinostroenie* [Heavy mechanical engineering]. No 7, p.p. 18-21.
8. Krushenko G.G. (2012) Poluchenie i primenenie poristyh metallicheskih materialov v tehnike [Production and application of porous metal materials in engineering]. *Vestnik Sibirskogo gosudarstvennogo ajerokosmicheskogo universiteta imeni akademika M. F. Reshetneva. Tehnologicheskie processy i materialy* [Bulletin of Siberian State Aerospace University. Technological processes and materials]. p.p. 181-184.
9. Tang H. P. (2012) Fractal dimension of pore-structure of porous metal materials made by stainless steel powder. *Powder Technology*. Vol. 217, p.p. 383-387.
10. Banhart J. (2000) Manufacturing routes for metallic foams. *Journal of metals*. Vol. 52, p.p. 22-27.
11. Nielsen H., Hufnagel W., Ganoulis G. (1974) Aluminium-Zentraie Düsseldorf. 1054 p.
12. Saenz E., Baranda P. S., Bonhomme J. (1998) Porous and cellular materials for structural applications. *Materials of Symp. Proc.* Vol. 521, p. 83.
13. Pavlenko A., Koshlak H. (2015) Production of porous material with projected thermophysical characteristics. *Metallurgical and Mining Industry*. No 1, p.p. 123 – 127.